# Synergistic Photocatalytic Degradation and Hydrogen Production Performances of $MWO_4$/tubular g-$C_3N_4$ Composites

Nurseli Görener Erdem[1], Özlem Tuna[2], and Esra Bilgin Simsek[1,*]

[1]Department of Chemical Engineering, Faculty of Engineering, Gebze Technical University, Kocaeli, Türkiye
[2]Department of Chemical Engineering, Faculty of Engineering, Yalova University, Yalova, Türkiye
Email: ngorener@gtu.edu.tr (N.G.E.); ozlem.tuna@yalova.edu.tr (O.T.); ebilgin@gtu.edu.tr (E.B.S.)
*Corresponding author

Manuscript received February 26, 2025; revised March 31, 2025; accepted May 14, 2025; published September 18, 2025

***Abstract*—In this work, a series of heterojunction composites including $MWO_4$ (M: Ce, Cu, Co) and tubular-shaped graphitic carbon nitride were synthesized as efficient photocatalysts towards degradation of tetracycline antibiotic under visible light irradiation. The results showed that the hybridization of materials significantly an enhanced the photocatalytic decomposition activity in which removal rates were found as 90%, 88% and 89% for $CuWO_4$/CN, $CoWO_4$/CN and $CeWO_4$/CN compared to that of pure CN (44%) after visible light irradiation for 2 h. Moreover, the photocatalytic hydrogen production rates were significantly enhanced after hybridization of the materials. The enhanced photocatalytic activity of $MWO_4$/CN composites was attributed to the Z-scheme transfer mechanism, which reduced recombination through the identical interaction among the energy bands of materials. Both characterization and photocatalytic performance tests demonstrated that the $MWO_4$/CN composites were successfully prepared with excellent activity and recyclability.**

***Keywords*—carbon nitride, metal tungstate, transition, photocatalysis, antibiotic**

## I. Introduction

Antibiotic contamination in water bodies has emerged as a critical environmental issue due to its potential to cause ecological damage and public health risks [1]. Among various antibiotics, tetracycline is one of the most widely used and frequently detected pollutants due to its extensive application in healthcare and agriculture [2]. Conventional methods for treating antibiotic-contaminated water are often insufficient, necessitating the development of advanced and sustainable approaches. Photocatalysis, driven by visible light, has garnered significant attention as an efficient and environmentally friendly method for degrading organic pollutants, including antibiotics [3].

Heterojunction photocatalysts offer promising potential for enhancing photocatalytic efficiency due to their ability to facilitate charge separation and suppress electron-hole recombination [4]. Graphitic carbon nitride (g-$C_3N_4$) has been widely studied for its visible-light-driven photocatalytic properties. Yet, its performance is often limited by fast charge recombination and a narrow range of light absorption [5]. To overcome these limitations, coupling g-$C_3N_4$ with suitable transition metal tungstates ($MWO_4$) to form heterojunction composites can provide a synergistic effect that enhances photocatalytic activity.

In this study, a series of heterojunction composites combining tubular-shaped graphitic carbon nitride and transition metal tungstates ($MWO_4$, M=Ce, Cu, Co) were synthesized and evaluated as visible-light photocatalysts for tetracycline degradation. This work highlights the significant improvement in photocatalytic performance achieved through material hybridization, providing insights into the Z-scheme transfer mechanism underlying the enhanced activity.

## II. Literature Review

The degradation of organic pollutants using photocatalytic systems has been a prominent area of research due to the increasing need for sustainable and efficient water purification technologies. Among the various materials studied, graphitic carbon nitride (g-$C_3N_4$) has gained significant attention because of its unique electronic properties, stability under visible light, and environmental friendliness. However, pristine g-$C_3N_4$ often suffers from drawbacks such as limited light absorption range, high charge carrier recombination rates, and moderate photocatalytic activity. To address these issues, researchers have explored strategies to modify or couple g-$C_3N_4$ with other materials to enhance its photocatalytic efficiency.

Metal tungstates ($MWO_4$) are another class of materials that have been investigated for photocatalytic applications due to their suitable bandgap structures and excellent stability [6, 7]. Studies have shown that the hybridization of g-$C_3N_4$ with transition metal tungstates, such as $CuWO_4$, $CoWO_4$, and $CeWO_4$, can form heterojunction systems with improved charge separation and extended light absorption capabilities. For instance, $CuWO_4$ has been reported to possess strong absorption in the visible region [8], while $CoWO_4$ exhibits excellent charge carrier mobility [9]. Similarly, $Ce_2(WO_4)_3$ has unique energy band alignments that facilitate effective charge transfer via redox cycle features of cerium [10, 11].

Recent studies have emphasized the role of Z-scheme heterojunctions in enhancing photocatalytic performance [12]. Z-scheme systems offer a mechanism that maintains the high redox potential of both semiconductors by enabling directional charge transfer while minimizing charge recombination [9]. This mechanism has been widely applied in heterojunction composites involving g-$C_3N_4$ and metal oxides or tungstates [13]. For example, research by Vinesh *et al.* [14] demonstrated that $CuWO_4$/g-$C_3N_4$ composites achieved a significant improvement in pollutant degradation under visible light compared to their components. Similarly, $CoWO_4$/g-$C_3N_4$ and $CeWO_4$/g-$C_3N_4$ composites could show

enhanced photocatalytic activity due to synergistic effects arising from their hybrid structures.

Despite these advancements, further research is needed to optimize the synthesis methods, understand the mechanistic details, and evaluate the recyclability and stability of these composites. This study builds on existing literature to evaluate and compare the photocatalytic performances of $MWO_4$/g-$C_3N_4$ composites, contributing valuable insights into their photocatalytic potential in both pollutant degradation and hydrogen evolution systems.

## III. Materials and Methods

### A. Preparation of Catalysts

Pristine tubular-shaped graphitic carbon nitride (g-$C_3N_4$) was synthesized using a hydrothermal method as described in [15]. In this process, melamine was dissolved in 40 mL of distilled water and stirred continuously for 30 min. The pH of the solution was then adjusted to 1 using phosphoric acid. The mixture was transferred into a Teflon-lined stainless steel hydrothermal reactor and maintained at 180 °C for 12 h. After cooling to room temperature, the resulting product was filtered, washed multiple times with distilled water, and dried. The sample was subsequently placed in a semi-closed crucible and calcined at 550 °C for 4 h with a heating rate of 3 °C/min. The final product was designated as CN.

Pristine $CuWO_4$ was synthesized using a co-precipitation method as described in [8]. A specified amount of $Na_2WO_4{\cdot}2H_2O$ and $CuSO_4{\cdot}5H_2O$ was dissolved in distilled water while stirring vigorously for 1.5 h. The resulting precipitate was then filtered and washed several times with distilled water. After drying, the sample was placed in an alumina crucible and calcined at 550 °C for 2 h in an air atmosphere. The final product was labeled as $CuWO_4$.

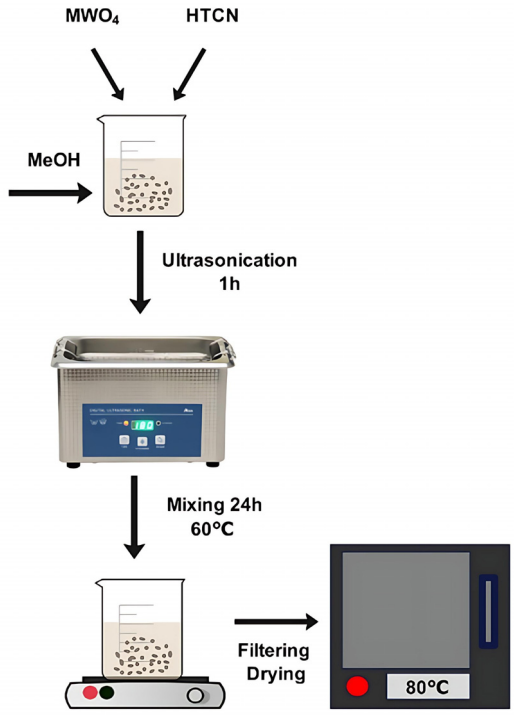


Fig. 1. Hybridization of $MWO_4$ with CN.

Cerium tungstate ($Ce_2(WO_4)_3$) catalyst was synthesized via a co-precipitation method followed by calcination. In this process, $Na_2WO_4{\cdot}2H_2O$ and $Ce(NO_3)_3{\cdot}6H_2O$ were dissolved in distilled water, and the pH of the solution was adjusted to 10.0 using $NH_4OH$. The mixture was stirred, and the resulting suspension was then vacuum filtered, and the precipitates were washed and dried in an oven. The white powders were placed in a crucible and calcined at 550 °C for 4 h. The final product was labeled as $CeWO_4$.

Pristine $CoWO_4$ was synthesized using a hydrothermal method as described in [16]. $CoCl_2{\cdot}6H_2O$ and $Na_2WO_4{\cdot}2H_2O$ were separately dissolved in distilled water. The two solutions were then combined, and the pH was adjusted to 10 using ammonia ($NH_3$). The resulting mixture was stirred continuously before being transferred into a stainless-steel autoclave for hydrothermal treatment at 180 °C for 18 h. Following the treatment, the mixture was vacuum-filtered and rinsed thoroughly with distilled water. The product was dried and subsequently calcined at 700 °C for 3 h to eliminate impurities.

$MWO_4$/CN hybrid catalysts were prepared using an ultrasound-assisted thermal impregnation method as shown in Fig. 1.

### B. Characterization

To characterize the as-synthesized photocatalysts, different characterization techniques were applied. The morphological properties and the elemental characterization of synthesized samples were studied scanning electron microscope (SEM) in conjunction with Energy Dispersive Spectroscopy (EDS) (Philips XL30 SFEG, Netherlands). X-Ray diffraction pattern (XRD) was obtained by Rigaku D-Max 2200 (Japan). The spectral characteristics of materials were investigated by UV–Vis diffuse reflectance spectra (DRS) using UV–VIS spectrometer (Shimadzu UV-2101, Japan). The photogenerated charge pair separation efficiencies were examined by the photoluminescence (PL, Varian Eclipse, USA) technique.

### C. Photocatalytic Tests

Photocatalytic performances of the as-synthesized materials were assessed by the photocatalytic decomposition of tetracycline as a target antibiotic contaminant under visible light irradiation. Two halogen lamps (with a wavelength of 400–700 nm) were used as a source of visible light. In a typical experiment, a specific dosage (0.05 g) of photocatalyst sample was dispersed into 30 ml of antibiotic solution (initial concentration of 10 mg/l) at an initial pH of 6.5 and then stirred in the dark for 30 min (to reach adsorption–desorption state). After switching the light on, the remaining antibiotic solution samples were taken from the reaction solution at time intervals to calculate the final concentration of tetracycline using a UV spectrophotometer.

Photocatalytic hydrogen evolution experiments were carried out using a quartz glass reactor. In each experiment, 100 mg of the catalyst was added to a solution of triethanolamine (TEOA, 1 g/L). The mixture was kept in a dark environment for 30 min to establish adsorption-desorption equilibrium before being exposed to visible light for 5 h to facilitate hydrogen production. The evolved hydrogen was quantified using gas chromatography equipped with a Carboxen column, a Thermal Conductivity Detector (TCD), and nitrogen as the carrier gas.

## IV. Results and Discussion

### A. Characterization

The micromorphology and microstructure of the as-synthesized materials were examined using SEM analysis, with the resulting images displayed in Fig. 2. The g-$C_3N_4$ catalyst exhibited a morphology of hollow tubular structure. Upon constructing the $CuWO_4$/HTCN heterostructure, the SEM images revealed that the $CuWO_4$ particles were closely adhered to the tubular surface of CN, establishing intimate surface contact. In contrast, the micrograph of the $CeWO_4$/CN heterostructure catalyst revealed that the spherical cerium tungstate nanoparticles were evenly distributed across the surface of the carbon nitride layers. The image of the $CoWO_4$/CN composite revealed that the cobalt tungstate perovskite particles were successfully anchored onto the surface of the tubular carbon nitride, highlighting the presence of strong interfacial interactions between the two components. This configuration may facilitate efficient charge transfer between the components due to the observed intimate physical contact; however, further confirmation of strong interfacial interactions would require additional analysis such as high-resolution TEM or XPS.

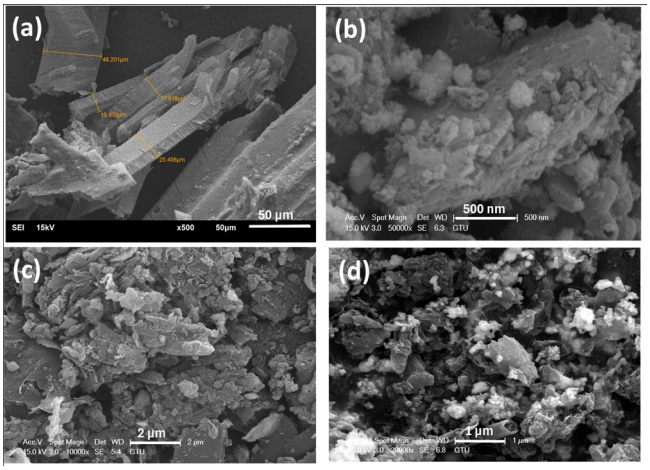


Fig. 2. SEM images of (a) bare CN, (b) $CeWO_4$/CN, (c) $CuWO_4$/CN (d) $CoWO_4$/CN.

The crystal structure and phase purity of as-fabricated catalysts were investigated by XRD analysis, and the diffraction patterns of each sample are demonstrated in Fig. 3. In the pattern of bare CN (Fig. 3(a)), the characteristic peak at 27.8° (002) was observed revealing its successful synthesis. Moreover, the strong and sharp peaks observed in all patterns indicate the high crystalline nature of as-synthesized composites (Fig. 3(b)). The crystallinity of $CoWO_4$/CN, $CoWO_4$/CN, and $CeWO_4$/CN was determined as 97.7%, 94.3%, and 60.2%, respectively. The dense peak pattern in the $CuWO_4$/CN XRD profile is due to the triclinic symmetry of $CuWO_4$ (JCPDS No: 01-070-1732), which results in multiple diffraction planes [17]. No extra peaks corresponding to impurities were detected, indicating phase purity after hybridization. Meanwhile, the wolframite monoclinic structure of $CoWO_4$ was observed in the hybrid structure (JCPDS card no: 00-15-0867) [18].

On the other hand, the major diffraction peaks in the XRD pattern of $CeWO_4$/CN revealed the monoclinic structure of cerium tungstate (JCPDS card no: 00-31-0340) [19]. Moreover, it is also worth noting that pristine g-$C_3N_4$ has only one major characteristic peak located at 27.8° corresponding to (002) (JCPDS card no: 50-1512) plane due to interplane stacking of the conjugated aromatic system of g-$C_3N_4$ [18].

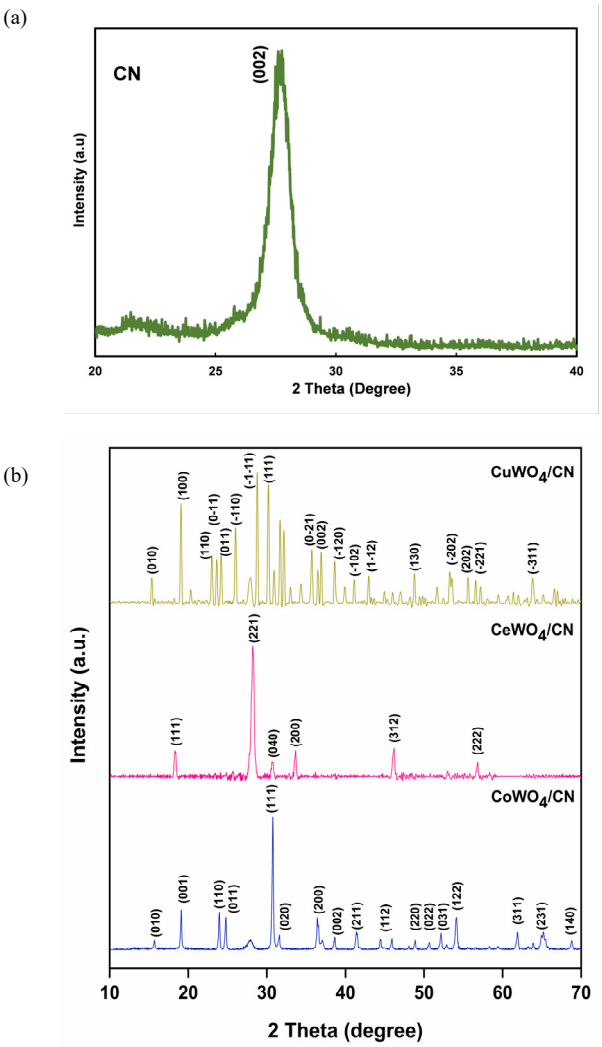


Fig. 3. XRD patterns of (a) bare CN and (b) hybrid samples.

Table 1. Band gap energy values of samples

| Catalyst | Band gap energy (eV) |
|---|---|
| CN | 2.70 |
| $CuWO_4$ | 2.35 |
| $CuWO_4$/CN | 2.70 |
| $CoWO_4$ | 2.60 |
| $CoWO_4$/CN | 2.90 |
| $Ce_2(WO_4)_3$ | 3.15 |
| $Ce_2(WO_4)_3$/CN | 3.05 |

The UV-DRS results provide insights into the optical properties of the catalysts by determining their band gap energies, which influence their light absorption capabilities. The calculated band gap energies are shown in Table 1. The pristine graphitic Carbon Nitride (CN) exhibited a band gap of 2.70 eV, enabling it to absorb visible light effectively, while the bare $CuWO_4$ has a smaller band gap (2.35 eV) compared to CN, making it more suitable for harvesting visible light. This lower band gap facilitated improved charge carrier generation under visible light irradiation. After hybridization, the composite of $CuWO_4$ and CN retains the band gap of CN as 2.70 eV, indicating that while the visible

light absorption capability of CN is preserved, the synergistic effect between $CuWO_4$ and CN enhances charge transfer efficiency, boosting photocatalytic activity. On the other hand, the pristine $CoWO_4$ has a band gap (2.60 eV) slightly narrower than CN, allowing it to absorb light in a similar range but with improved separation of charge carriers due to its unique electronic structure. After hybridization, the band gap of the $CoWO_4$/CN composite (2.90 eV) was slightly larger than that of CN and $CoWO_4$. This increase suggested enhanced structural interactions that may improve photoinduced electron-hole pair separation, despite a slight reduction in visible light absorption. In case of cerium-based catalysts, $Ce_2(WO_4)_3$ had the largest band gap (3.15 eV) among the catalysts, restricting its absorption to the UV region and limiting its visible light utilization. The incorporation of CN into $Ce_2(WO_4)_3$ reduced the band gap slightly (3.05 eV), extending light absorption into the near-visible range and improving its photocatalytic potential. The optical results demonstrated the tunability of the band gap energy by forming composites with CN, which can enhance the photocatalytic activity through better charge separation and light absorption, depending on the composition and interaction of the materials.

### *B. Photocatalytic Removal Tests*

The catalytic activities of pristine materials and as-fabricated binary composites were evaluated for visible light-driven tetracycline degradation. As shown in Fig. 4, the bare CN, $Ce_2(WO_4)_3$, $CuWO_4$, and $CoWO_4$ achieved degradation efficiencies of 41%, 54.8%, 54.7%, and 53.5%, respectively. However, the incorporation of metal tungstate catalysts with tubular-shaped carbon nitride significantly enhanced the decomposition performance. The removal efficiency increased to 89.9%, 90.2%, and 88.5% for $CeWO_4$/CN, $CuWO_4$/CN, and $CoWO_4$/CN, respectively. The hybridization with carbon nitride could enhance the functional active sites, tune the band-gap structure, and suppress charge recombination, resulting in improved catalytic activity. It is important to note that photocatalytic activity is not governed solely by band gap energy. Despite $CeWO_4$/CN having a larger band gap (3.05 eV), its superior degradation performance can be attributed to improved redox potential and effective charge separation due to the Z-scheme heterostructure. This underscores the synergistic effects of interfacial charge transfer, surface properties, and optical features beyond mere band gap considerations.

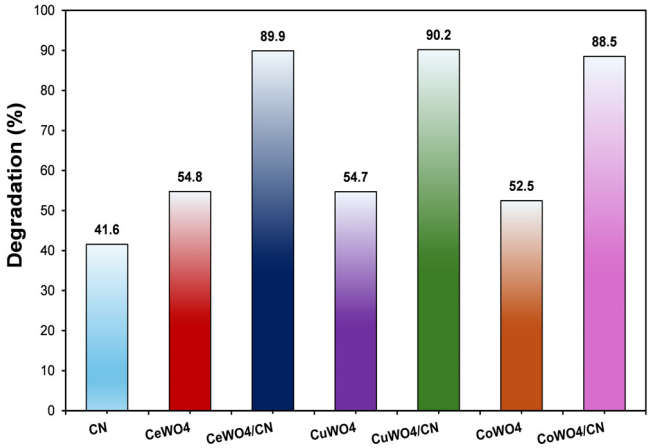


Fig. 4. Photocatalytic degradation performances of the samples.

The influence of the peroxymonosulfate (PMS) as Fenton agent on the tetracycline degradation was investigated and the results are shown in Fig. 5. Apparently, the degradation rate of TC increased with the addition of PMS and the removal rates of $CeWO_4$/CN, $CuWO_4$/CN, and $CoWO_4$/CN were observed as 98.8%, 93.7% and 92.3%, respectively. The enhanced performance was attributed to the generation of highly reactive sulfate and hydroxyl radicals through the activation of PMS, which accelerated the breakdown of tetracycline molecules. These findings indicated that PMS acts as an effective co-catalyst, boosting the catalytic activity of the composites by promoting reactive oxygen species formation and facilitating the degradation process.

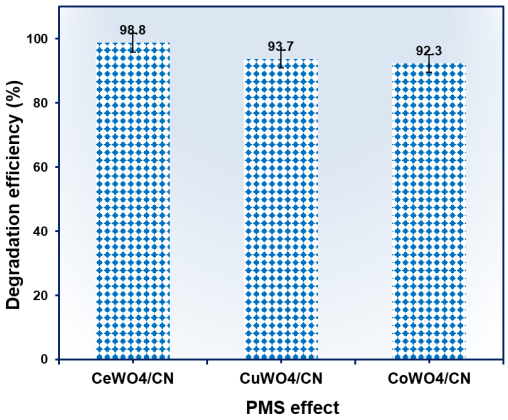


Fig. 5. Effect of PMS on the TC removal efficiencies.

The effect of hydrogen peroxide ($H_2O_2$) as a Fenton agent on tetracycline degradation was examined, and the results are shown in Fig. 5. The addition of $H_2O_2$ significantly enhanced the degradation rate, achieving removal efficiencies of 90.4%, 92.0%, and 89.6% for $CeWO_4$/CN, $CuWO_4$/CN, and $CoWO_4$/CN, respectively. This improvement is attributed to the generation of highly reactive hydroxyl radicals via $H_2O_2$ activation, which accelerated the breakdown of tetracycline molecules. These results highlight the role of $H_2O_2$ as an effective co-catalyst, improving the catalytic performance of the composites by boosting the formation of reactive oxygen species and facilitating the degradation process.

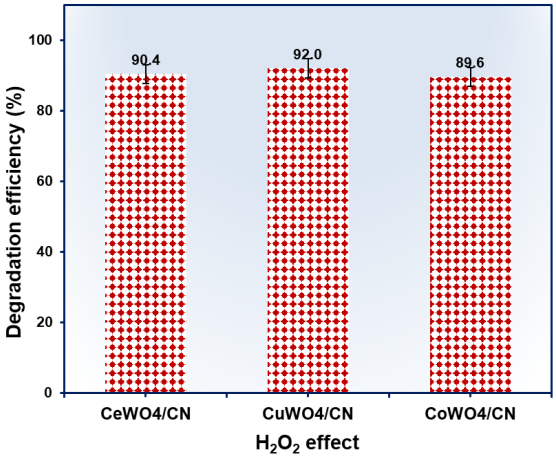


Fig. 6. Effect of $H_2O_2$ on the TC removal efficiencies.

### *C. Hydrogen Production Performances*

The photocatalytic hydrogen production performances of $CuWO_4$/CN and $CoWO_4$/CN composites were evaluated

under visible light irradiation (Fig. 7). The $CeWO_4$/CN composite was not tested for hydrogen evolution due to the relatively positive conduction band position of $Ce_2(WO_4)_3$, which limits its ability to participate in photocatalytic hydrogen generation, even under visible light excitation. The bare carbon nitride exhibited a low hydrogen production performance of 4,909 μmol/gcat. Both materials demonstrated notable hydrogen evolution rates due to their efficient charge separation and strong light-harvesting capabilities. $CuWO_4$/CN exhibited higher activity as 12,688 μmol/gcat, than the bare $CuWO_4$ (5,741 μmol/gcat), which was attributed to the synergistic interaction between $CuWO_4$ and carbon nitride, which facilitated enhanced electron transfer and reduced recombination of photogenerated charge carriers. Similarly, $CoWO_4$/CN showed superior hydrogen production performance as 9,984 μmol/gcat, benefiting from the improved catalytic properties of $CoWO_4$ and the optical and structural advantages of carbon nitride. The results indicate that these composites effectively utilize solar energy for hydrogen generation, showcasing their potential as sustainable photocatalysts for clean energy applications.

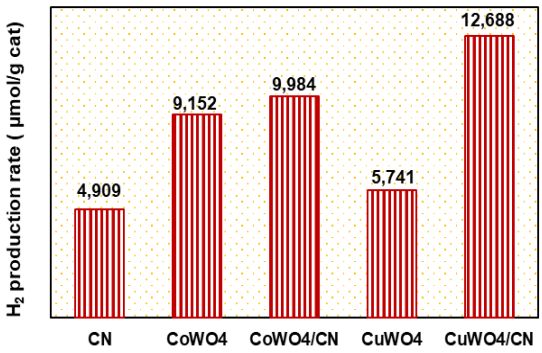

Fig. 7. Photocatalytic hydrogen evolution performances.

### D. Photocatalytic Reaction Mechanism

Considering the characterization and experimental results, possible photocatalytic reaction mechanism was proposed as: Upon visible light irradiation, both g-$C_3N_4$ and $MWO_4$ (M=Cu, Co) semiconductors absorb photons, leading to the excitation of electrons from the Valence Band (VB) to the Conduction Band (CB), and consequently generating electron–hole ($e^-/h^+$) pairs. Due to the construction of a direct Z-scheme heterojunction between the two components, the photogenerated electrons in the conduction band of $MWO_4$ preferentially recombine with the holes in the valence band of g-$C_3N_4$ at the interface. This charge transfer pathway differs fundamentally from traditional Type-II heterojunctions. In the Z-scheme system, the remaining electrons in the CB of g-$C_3N_4$ retain strong reducing power (with a CB position more negative than 0 V vs. NHE), while the holes in the VB of $MWO_4$ maintain high oxidation potential. These separated charge carriers participate in subsequent redox reactions, enabling photocatalysis.

For pollutant degradation, the oxidative holes on $MWO_4$ can directly oxidize tetracycline molecules or react with $H_2O/OH^-$ to form hydroxyl radicals (•OH), which are highly reactive species capable of breaking down organic contaminants. Simultaneously, the photogenerated electrons in g-$C_3N_4$ reduce molecular oxygen ($O_2$) into superoxide radicals ($•O_2^-$), further contributing to oxidative degradation through a synergistic mechanism.

For hydrogen evolution, the retained photogenerated electrons on the CB of g-$C_3N_4$ are energetic enough to reduce protons ($H^+$) in aqueous triethanolamine (TEOA) solution to generate molecular hydrogen ($H_2$). This is feasible only when the CB potential of the semiconductor lies above the $H^+/H_2$ reduction potential (0 V vs. NHE), as is the case for CN and (Cu/Co)$WO_4$-based systems.

## V. Conclusion

In this study, a series of heterojunction composites combining tubular-shaped graphitic carbon nitride (g-$C_3N_4$) with transition metal tungstates ($MWO_4$, M = Ce, Cu, Co) was successfully synthesized and evaluated as visible-light photocatalysts for the degradation of tetracycline antibiotic. The results demonstrated a significant enhancement in photocatalytic performance compared to pure g-$C_3N_4$. The enhanced activity of these composites was attributed to the Z-scheme charge transfer mechanism, which effectively reduced charge recombination and maintained high redox potentials. Comprehensive characterization and performance tests confirmed the successful synthesis of the $MWO_4$/g-$C_3N_4$ composites, showcasing their excellent stability, recyclability, and potential for practical environmental applications.

This work highlights the potential of $MWO_4$/g-$C_3N_4$ heterojunctions as efficient and sustainable photocatalysts for water purification, paving the way for further advancements in the development of innovative materials for environmental remediation. Future studies should focus on fine-tuning the material properties and exploring their applications in broader pollutant degradation scenarios.

## Conflict of Interest

The authors declare no conflict of interest.

## Author Contributions

Nurseli Gorener Erdem: Investigation, Data curation, Writing, Özlem Tuna: Methodology, Investigation, Writing, Esra Bilgin Simsek: Conceptualization, Supervision, Project administration, Resources, Writing; all authors had approved the final version.

## Funding

This research was funded by Gebze Technical University Research Universities Support Program (ADEP) with the Project Number 2024-A-113-07.

## References

[1] K. Liu, Z. Tong, Y. Muhammad, G. Huang, H. Zhang, Z. Wang, Y. Zhu, and R. Tang, "Synthesis of sodium dodecyl sulfate modified BiOBr/magnetic bentonite photocatalyst with three-dimensional parterre like structure for the enhanced photodegradation of tetracycline and ciprofloxacin," *Chem. Eng. J.*, vol. 388, 124374, 2020. DOI: 10.1016/j.cej.2020.124374

[2] V. Varadharajan, D. S. Senthilkumar, K. Senthilkumar, V. P. Sundramurthy, R. Manikandan, H. Senthilarasan, H. Ganesan, I. Kesavamoorthy, and A. Ramasamy, "Process modeling and toxicological evaluation of adsorption of tetracycline onto the magnetized cotton dust biochar," *J. Water Process Eng.*, vol. 49, pp. 103046, 2022. DOI: 10.1016/j.jwpe.2022.103046

[3] D. P. H. Tran, M. T. Pham, Y. F. Wang, T. C. Chang, and S. J. You, "Tuning visible light-driven photocatalytic NO removal: Insights from glucose-derived CQDs/ZnO nanorods composite," *J. Environ. Chem. Eng.*, vol. 11, 111561, 2023. DOI: 10.1016/j.jece.2023.111561

[4] Y. He, J. Huang, B. Wang, and Y. Qu, "Construction of Z-scheme heterojunction C3N4/N-CQDs@W18O49 for full-spectrum photocatalytic organic pollutant degradation," *Appl. Surf. Sci.*, vol. 610, 155255, 2023. DOI: 10.1016/j.apsusc.2022.155255

[5] G. Zhou, L. Meng, X. Ning, W. Yin, J. Hou, Q. Xu, J. Yi, S. Wang, and X. Wang, "Switching charge transfer of g-$C_3N_4$/$BiVO_4$ heterojunction from type II to Z-scheme via interfacial vacancy engineering for improved photocatalysis," *Int. J. Hydrogen Energy*, vol. 47, pp. 3014–3026, 2022. DOI: 10.1016/j.ijhydene.2021.12.226

[6] T. Montini, V. Gombac, A. Hameed, L. Felisari, G. Adami, and P. Fornasiero, "Synthesis, characterization and photocatalytic performance of transition metal tungstates," *Chem. Phys. Lett.*, vol. 498, pp. 113–119, 2010. DOI: 10.1016/j.cplett.2010.08.026

[7] U. M. García-Pérez, A. Martínez-De La Cruz, and J. Peral, "Transition metal tungstates synthesized by co-precipitation method: Basic photocatalytic properties," *Electrochim. Acta*, vol. 81, pp. 227–232, 2012. DOI: 10.1016/j.electacta.2012.07.045

[8] A. Sarwar, A. Razzaq, M. Zafar, I. Idrees, F. Rehman, and W. Y. Kim, "Copper tungstate (CuWO4)/graphene quantum dots (GQDs) composite photocatalyst for enhanced degradation of phenol under visible light irradiation," *Results Phys.*, vol. 45, 106253, 2023. DOI: 10.1016/j.rinp.2023.106253

[9] H. Yang, J. Li, Q. Su, B. Wang, Z. Zhang, Y. Dai, Y. Li, and L. Hou, "Construction of $Bi_2MoO_6$/$CoWO_4$ Z-scheme heterojunction for high-efficiency photocatalytic degradation of norfloxacin under visible light: Performance and mechanism insights," *Chem. Eng. J.*, vol. 470, 144139, 2023. DOI: 10.1016/j.cej.2023.144139

[10] A. Jose, M. John, H. Hitha, S. Kuriakose, K. P. Baiju, and T. Varghese, "Characterization of $Ce_2(WO_4)_3$ nanocrystals for potential applications," *Results in Surfaces and Interfaces*, vol. 4, 100020, 2021. DOI: 10.1016/j.rsurfi.2021.100020

[11] G. Ahilandeswari and D. Arivuoli, "Investigation of $Ce_2(WO_4)_3$/g-$C_3N_4$ nanocomposite for degradation of industrial pollutants through sunlight-driven photocatalysis," *Appl. Phys. A Mater. Sci. Process.*, vol. 128, pp. 1–16, 2022. DOI: 10.1007/s00339-022-05846-w

[12] Y. Qiu, Z. Xing, M. Guo, Z. Li, N. Wang, and W. Zhou, "Hollow cubic $Cu_2$-xS/Fe-POMs/$AgVO_3$ dual Z-scheme heterojunctions with wide-spectrum response and enhanced photothermal and photocatalytic-fenton performance," *Appl. Catal.. B Environ.*, vol. 298, 120628, 2021. DOI: 10.1016/j.apcatb.2021.120628

[13] Y. Wu, X. Zhao, S. Huang, Y. Li, X. Zhang, G. Zeng, L. Niu, Y. Ling, and Y. Zhang, "Facile construction of 2D g-$C_3N_4$ supported nanoflower-like NaBiO3 with direct Z-scheme heterojunctions and insight into its photocatalytic degradation of tetracycline," *J. Hazard. Mater.*, vol. 414, 125547, 2021. DOI: 10.1016/j.jhazmat.2021.125547

[14] V. Vinesh, M. Preeyanghaa, T. R. N. Kumar, M. Ashokkumar, C. L. Bianchi, and B. Neppolian, "Revealing the stability of CuWO4/g-C3N4 nanocomposite for photocatalytic tetracycline degradation from the aqueous environment and DFT analysis," *Environ. Res.*, vol. 207, 112112, 2022. DOI: 10.1016/j.envres.2021.112112

[15] Ö. Tuna, H. H. Mert, M. S. Mert, and E. Bilgin Simsek, "Tailoring the surface features of CaWO4 by coupling with tubular g-$C_3N_4$ for enhanced solar photocatalysis and thermal energy storage," *J. Energy Storage*, vol. 86, 111398, 2024. DOI: 10.1016/j.est.2024.111398

[16] H. Ashiq, N. Nadeem, A. Mansha, J. Iqbal, M. Yaseen, M. Zahid, and I. Shahid, "G-$C_3N_4$/Ag@$CoWO_4$: A novel sunlight active ternary nanocomposite for potential photocatalytic degradation of rhodamine B dye," *J. Phys. Chem. Solids*, vol. 161, 110437, 2022. DOI: 10.1016/j.jpcs.2021.110437

[17] R. Gupta, B. Boruah, J. M. Modak, and G. Madras, "Kinetic study of Z-scheme C3N4/CuWO4 photocatalyst towards solar light inactivation of mixed populated bacteria," *J. Photochem. Photobiol. A Chem.*, vol. 372, pp. 108–121, 2019. DOI: 10.1016/j.jphotochem.2018.08.035

[18] S. L. Prabavathi, K. Govindan, K. Saravanakumar, A. Jang, and V. Muthuraj, "Construction of heterostructure $CoWO_4$/g-$C_3N_4$ nanocomposite as an efficient visible-light photocatalyst for norfloxacin degradation," *J. Ind. Eng. Chem.*, vol. 80, pp. 558–567, 2019. DOI: 10.1016/j.jiec.2019.08.035

[19] H. M. Altass, M. Morad, A. S. Khder, M. Raafat, R. I. Alsantali, M. A. Khder, R. S. Salama, M. Shaheer Malik, Z. Moussa, M. A. S. Abourehab, and S. A. Ahmed, "Exploitation of the unique acidity of novel cerium-tungstate catalysts in the preparation of indole derivatives under eco-friendly acid-catalyzed Fischer indole reaction protocol," *Arab. J. Chem.*, vol. 15, 103670, 2022. DOI: 10.1016/j.arabjc.2021.103670